THE ANALYST
FULL PAPER
www.rsc.org/analyst

Light emitting diode excitation emission matrix fluorescence spectroscopy

Sean J. Hart* and Renée D. JiJi†

Naval Research Laboratory, Chemistry Division, Biological Chemistry, Code 6113, 4555 Overlook Ave, S.W, Washington, DC 20375, USA. E-mail: shart@ccf.nrl.navy.mil; Fax: (202) 404-8119; Tel: (202) 404-3361

Received 6th August 2002, Accepted 21st October 2002
First published as an Advance Article on the web 7th November 2002

An excitation emission matrix (EEM) fluorescence instrument has been developed using a linear array of light emitting diodes (LED). The wavelengths covered extend from the upper UV through the visible spectrum: 370–640 nm. Using an LED array to excite fluorescence emission at multiple excitation wavelengths is a low-cost alternative to an expensive high power lamp and imaging spectrograph. The LED-EEM system is a departure from other EEM spectroscopy systems in that LEDs often have broad excitation ranges which may overlap with neighboring channels. The LED array can be considered a hybrid between a spectroscopic and sensor system, as the broad LED excitation range produces a partially selective optical measurement. The instrument has been tested and characterized using fluorescent dyes: limits of detection (LOD) for 9,10-bis(phenylethynyl)-anthracene and rhodamine B were in the mid parts-per-trillion range; detection limits for the other compounds were in the low parts-per-billion range (< 5 ppb). The LED-EEMs were analyzed using parallel factor analysis (PARAFAC), which allowed the mathematical resolution of the individual contributions of the mono- and dianion fluorescein tautomers *a priori*. Correct identification and quantitation of six fluorescent dyes in two to six component mixtures (concentrations between 12.5 and 500 ppb) has been achieved with root mean squared errors of prediction (RMSEP) of less than 4.0 ppb for all components.

Introduction

Fluorescence excitation emission matrix (EEM) spectroscopy has long been known as a powerful method for complex mixture analysis.[1–3] The ability to easily collect full emission spectra for several excitation wavelengths, has generally required expensive and complex instrumentation. The multi-way characteristics of EEM data enable the extraction of the salient chemical features. As a consequence, mathematical resolution of analytes is possible, even in the presence of unknown interferences, which is known as the second-order advantage.[4] While a conventional fluorimeter can be used to collect EEM data, the process is neither quick nor automated. Furthermore, its size prevents use in applications where field portability is desired. For this reason, many research groups have developed alternative instrumentation for performing EEM spectroscopy.[5–10] The light source most commonly used for single measurement EEM spectroscopy is a lamp and spectrograph which have been rotated to vertically illuminate the sample cell with wavelength dispersed light.[5–7] The vertical illumination serves to allow the resulting spatially separated fluorescence spectra to be collected by a second spectrograph. Most commonly, a charge coupled device (CCD)[11] is used to image the resulting two-dimensional EEM spectrum. Other light sources have been utilized including a rapid scanning dye laser system,[3] and a laser Raman shifter system for remote EEM collection.[12–14]

In this paper, we describe a new method of single measurement EEM spectroscopy which is based upon an array of light emitting diodes (LED). The array of LEDs is focused into a sample cuvette, creating spatially separated excitation spots. Fluorescence from analytes in solution is collected at right angles by another lens, which images the fluorescent spots onto the entrance of a spectrograph with a CCD camera for detection. The broad emission spectrum of LEDs permits continuous coverage over a large excitation range with a limited number of LEDs, allowing excitation of all analytes with absorption within the LED's excitation range. From a sensors standpoint, LEDs can be viewed as multiple partially selective instrumental elements. These individual components, when combined, provide a more complete spectroscopic picture of the chemical puzzle. The success of low excitation resolution LED-EEM spectroscopy demonstrates that it is not always necessary to have high excitation wavelength resolution. In fact, the method performs well irrespective of the overlapping excitation wavelength regions. Unique excitation information is generated for even heavily overlapped excitation ranges. Each analyte may then be uniquely excited by each LED, thereby, conserving the multi-way characteristics of the data common to all EEM methods. This knowledge affords many concessions in the development of a spectroscopic sensor system: reduced size, cost, complexity, without sacrificing analytical performance.

The novel light source used with this method will allow a multitude of laboratories to easily begin collecting fluorescence EEMs. The cost of the traditional excitation source used in single measurement EEM spectroscopy, a lamp and spectrograph, is high: generally costing more than $10000. Researchers currently using a spectrograph and CCD camera, for fluorescence detection, can now easily and inexpensively achieve the multi-way advantages offered by EEM spectroscopy; the cost of an LED array excitation source is approximately $300. Future advances in LED technology may result in lower UV wavelengths being made available, thus extending the range of applications.

The use of LEDs in analytical chemical spectroscopy is burgeoning;[15–17] the advantages are many. LEDs require only a minimal voltage to produce a relatively significant quantity of light. For example, a blue (470 nm) LED driven by 3.79 V at 20 mA produces 1.1 mW of optical power. These electrical powers can easily be generated using batteries, which will allow this type of excitation source to eventually be portable. Addition-

† NRC-NRL Research Associate.

This journal is © The Royal Society of Chemistry 2002 **Vilber EX1050 1**

ally, the LEDs' outputs were very stable over the course of these experiments, eliminating the need for intensity correction methods which are necessary when using lamp and laser sources. Another advantage is that LEDs are small, 1–5 mm in diameter or length, and can be modified and affixed directly to optical elements or sample holders using epoxy.[17] This means that multiple LEDs can be fused to generate more excitation light if desired. The wavelength band widths can be large with typical full width half maximums between 10 nm and 50 nm or more. This reduces the chance of analyte absorption bands being missed as can happen with laser induced fluorescence. An additional advantage is the ability to customize the individual excitation wavelengths in the LED array.

The disadvantages associated with LED spectroscopy include the current lack of lower ultraviolet (UV) wavelengths, which limits the application to long wavelength UV, visible, and near-infrared (IR) excitable fluorescent compounds. The wide excitation band width can hamper the observation of small Stoke's shifted fluorescence which overlaps with the excitation band. The removal of scattered light may also be more difficult due to the wider bandwidth of the LEDs. This should not be a limiting feature as pre-processing methods including background subtraction and peak removal algorithms have been demonstrated as useful techniques for mitigating scattered light effects.[18] In addition, modeling background and scattered light features has been accomplished.[5,6]

The full range of molecules and dyes which fluoresce under long wavelength UV (370 nm) through near infra-red (NIR) wavelength (980 nm) excitation can be used with this inexpensive and simple to construct EEM system. The potential applications of upper UV, visible, and NIR fluorescence include fluorescence of dyes, larger PAHs (anthracene, chrysene, benzo[*a*]pyrene, perylene, *etc.*), humic materials,[19,20] chlorophylls from plants[21] and algae[22] and NIR fluorescence from bacteriochlorophyll[23] in certain bacteria. Others applications include environmental dye tracers[24,25] and porphyrin fluorescence.[26] Fluorescence of porphyrins and derivatives can be used for detection of certain cancers using patient sera analysis,[27] and as markers for heavy metal poisoning through urine analysis.[28]

Experimental

The LED-EEM instrument is composed of the excitation source, the sample chamber, and the detection system. The LEDs were focused into the sample chamber using a single lens to focus an image of the array into a fluorescence cuvette. Another lens was used to collect fluorescence at a right angle from the LED-array image and focus it onto the entrance plane of a spectrograph with subsequent detection using a CCD camera.

The LED light source was constructed in our lab as follows. The LEDs were driven by a linear DC power supply (SLS-05-030-1T, SOLA, Allied Electronics, Fort Worth, TX) connected to an individual potentiometer (part number 754-2172, Allied Electronics, Fort Worth, TX) for each LED. The 370 nm, 430 nm LEDs were obtained from Eastern Electronics (Springfield, VA, a distributor for Ledtronics, http://www.ledtronics.com) the 470 nm from Allied Electronics (Part #990-3384, Fort Worth, TX), and the remaining LEDs were obtained from The LED Light (505 nm LED, T13/4-20BL-GRN-a, 530 nm LED, T1-3/4-15G-a, 590 nm LED, T1-3/4-8YL, and 636 nm LED, T1-3/4-8RD, http://www.theledlight.com, Fallon, NV). A summary of the LED specifications used to construct the array is given in Table 1. The 5 mm diameter LEDs were mounted between two 15 mm × 70 mm prototyping boards (977–1255, Allied Electronics, Fort Worth, TX) which had been drilled out to accommodate each LED. The boards were held together using four bolts and nuts. Eight LEDs were spaced evenly at approximately 7 mm center to center, which resulted in a 57 mm long array, from the top LED to the bottom LED. One LED, fifth from the top, was not used as the wiring failed after installation in the electronics box. The optical powers (measured at the LED) reported in Table 1 were measured using both UV and visible detector heads (LM2-UV, LM2-VIS, Coherent, Auburn, CA) and a digital meter (Fieldmaster GS, Coherent, Auburn, CA). The LEDs were not all driven at the optimum voltages; the system was optimized with respect to the blue excitation spectrum due to the lower excitation intensities of those LEDs. The incident excitation powers, at the sample, were between 0.4% and 5% of the total optical power measured at the LED. These losses were worse in off-axis positions due to aberrations and vignetting. The actual LED wavelengths reported were measured using an Ocean Optics miniature spectrometer (S2000, Ocean Optics, Dunedin, FL) and a 200 μm optical fiber (Polymicro Technologies, Phoenix, AZ). Fig. 1 is a photograph of the illuminated LED array, showing the two prototyping boards which sandwich and thus support the back portion of each LED. The array was attached to a linear translating stage (part #16121, Thermo Oriel, Stratford, CT)

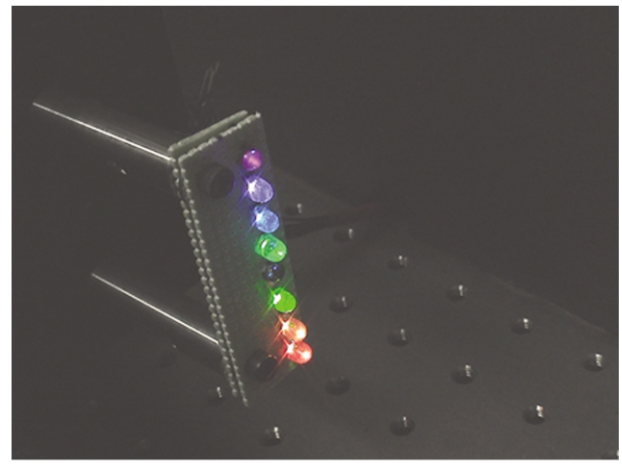

Fig. 1 Photograph of the illuminated LED array. The LEDs from top to bottom are 370 nm, 430 nm, 470 nm, 505 nm, unused LED, 530 nm, 590 nm, 636 nm.

Table 1 Array electrical and optical specifications

Nominal LED λ/nm	Actual LED λ/nm	Bandpass FWHM[a]/nm	Viewing angle/°	Forward voltage/V	Optical power/μW[b]
370	379.4	15	10	3.83	759
430	434.0	73	15	3.55	223
470	473.6	22	15	2.84	78
505	514.5	47	15	2.97	108
530	533.2	32	15	2.40	56
590	593.0	14	8	1.95	236
636	633.5	17	8	1.85	533

[a] FWHM—full width half maximum. [b] Measured at the LED.

using two optical posts. This allowed precise positioning of the array image, within the cuvette, and thus on the spectrograph entrance plane and CCD. The excitation bandpass of the LED system is unconventional and must be considered on a per channel basis. For our system the minimum bandpass was 14 nm and the maximum was 73 nm. The wavelength output distribution of the LED defines the bandpass for that channel. Fig. 2 contains the optical output of each LED as a function of wavelength, measured using the miniature spectrometer. Different LEDs of the same nominal wavelength, from the same manufacturer, had peak wavelengths which varied by less than 1%. Considering the large wavelength range of each LED, these represent relatively minor wavelength variations.

The sample was placed in a fluorescence cuvette (3/Q/10-GL14-C, Starna Cells Inc., Atascadero, CA), which was held in a cuvette holder (Part #13950, Thermo Oriel, Stratford, CT). The LED array image was focused into a sample cuvette using a 50 mm diameter, 50 mm focal length lens with a VIS-NIR anti-reflection coating (Part #A45-715, Edmund Industrial Optics, Barrington, NJ). An adjustable iris (Part NT32-619, Edmund Industrial Optics, Barrington, NJ) set at a 20 mm opening was placed between the array and the lens to limit off axis rays and stray light. An illustration of the instrument is shown in Fig. 3. A 25 mm diameter, 50 mm focal length lens with a VIS-NIR anti-reflection coating (Part #45-508, Edmund Industrial Optics, Barrington, NJ) was used to collect fluorescence at right angles to the LED excitation spots and image the fluorescence onto the entrance image plane of the spectrograph. The LED array was 430 mm from the excitation lens, and the fluorescence collection lens was 190 mm from the sample cuvette. These distances resulted in an appropriate reduction in the size of the LED array image which was imaged through the spectrograph slit.

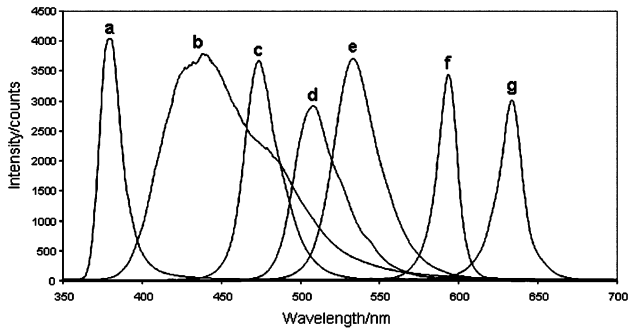

Fig. 2 LED output intensities as a function of wavelength, (a) 370 nm, (b) 430 nm, (c) 470 nm, (d) 505 nm, (e) 530 nm, (f) 590 nm, and (g) 636 nm.

The detection system consisted of a ¼ m imaging spectrograph (MS260i, Thermo Oriel, Stratford, CT) fitted with a removable 50 μm fixed slit and a 300 line/mm grating blazed at 500 nm resulting in a 1 nm emission bandpass. Mounted at the exit pane was a 1024 × 256 pixel CCD camera (Instaspec IV, Thermo Oriel, Stratford, CT), cooled to −55 °C. The integration time used throughout this work was 60 s, unless otherwise noted, and the dark current was subtracted in real time by the acquisition software (Instaspec, Thermo Oriel, Stratford, CT). In Fig. 3, the image was obtained by reflecting the array image toward the collection lens using a glass slide cut and placed in the cuvette at 45 degrees. As can be seen in the image data, in Fig. 3, each LED image is spatially separated along the vertical axis and is wavelength separated by the grating in the spectrograph along the horizontal axis. The CCD was binned by 10 pixels in the vertical direction, defining each excitation channel. Binning was chosen by observing the LED scattering spots measured by the CCD and selecting the ten best pixels to

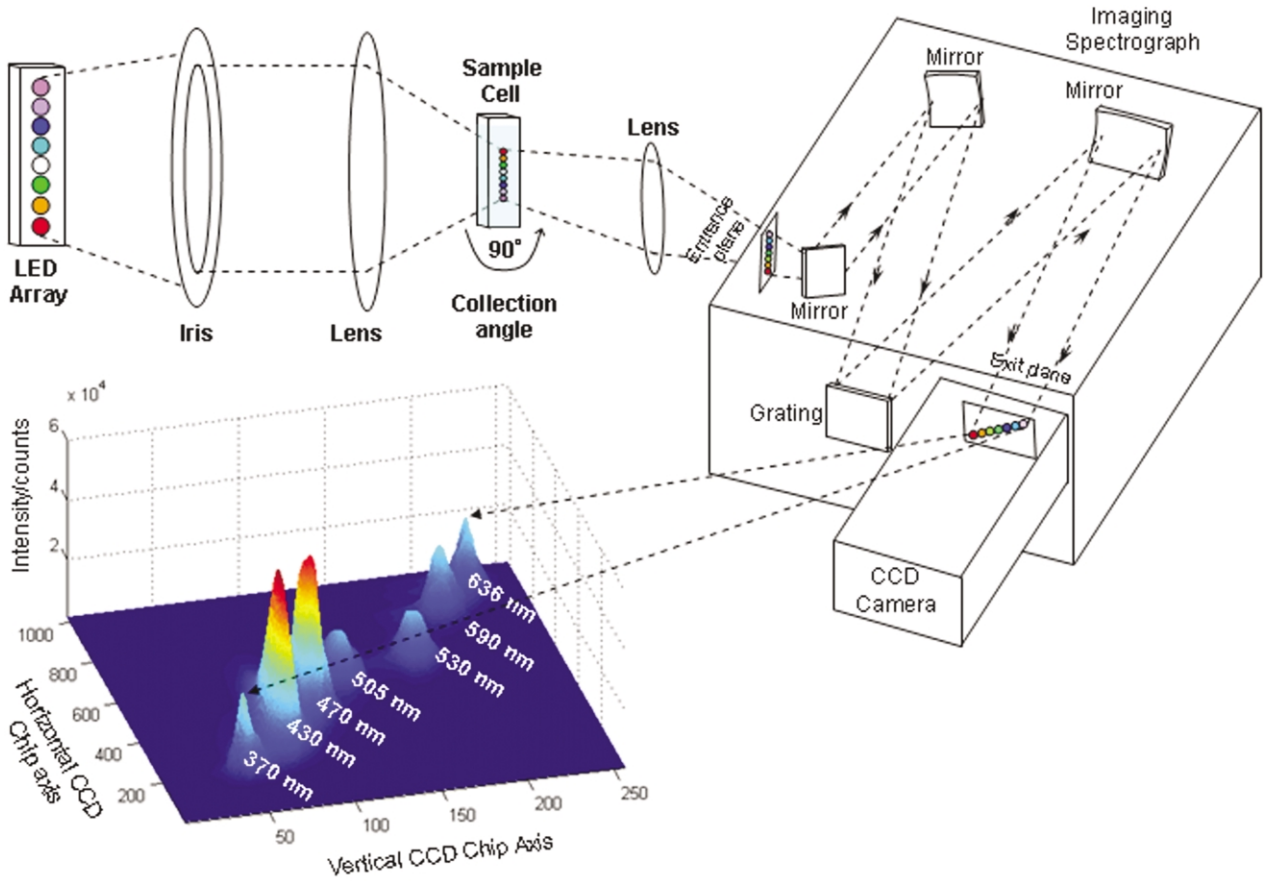

Fig. 3 Illustration of the LED-EEM instrument and full chip reflection image of the LED excitation spots. The light path through the system is drawn, showing the inversion of the LED array and the subsequent reflected image of the wavelength dispersed LED array. The grating center wavelength was 500 nm in this image.

collect data from each excitation spot. Seven 10 pixel sections, corresponding to each LED, of the CCD image were hardware binned in the vertical dimension producing 7 × 1024 LED-EEMs.

The data were collected using a 400 MHz Pentium PC and analyzed using PARAFAC code written in Matlab (The Mathworks, Natick, MA) based upon the theory described above.[30] The only preprocessing required was the removal of cosmic noise spikes, which was accomplished by calculating the derivative spectrum at each excitation wavelength and finding inflection points greater than 3σ, where σ equals the standard deviation of the derivative spectrum, and replacing them with the mean of the surrounding 10 points.

All analytes were dissolved in ultra pure reagent grade water (Alpha-Q, Millipore, Bedford, MA) or absolute ethanol (The Warner-Graham Company, Cockeysville, MD). Safranin O (99%), nile red, 9,10-diphenylanthracene (98%), fluorescein (95%), and 9,10-bis(phenylethynyl)-anthracene (97%) (Aldrich Chemical Company, Milwaukee, WI) were used without further purification. Rhodamine B, laser grade, (Acros Organics, NJ) was also used without further purification. All dyes were prepared in ethanol at concentrations between 12.5 and 500 ppb. A solution of a scattering standard, glycogen, 0.11% in water, was used to measure light scatter to quantify excitation stability in between analyte measurements. Four single analyte standard solutions of differing concentrations were prepared for each dye as well as 18 prediction samples containing between two and six dyes. Three replicate EEMs were collected for each sample. In addition, 50 replicate blank spectra (ethanol) were also measured throughout the data collection.

Figures of merit were calculated according to convention. Sensitivity was defined as the slope of the least squares fit of the data, the limit of detection (LOD) was determined as $3\sigma_b$, where σ_b is the standard deviation of the predicted concentration of the respective analyte in the blanks. The root mean squared errors of calibration (RMSEC) and prediction (RMSEP) for each analyte were calculated according to Eqn. (1),

$$\mathrm{RMSE} = \sqrt{\sum_{k=1}^{K} (c_k - \hat{c}_k)^2 / K} \qquad (1)$$

where K is the number of standards or unknowns, c_k and $\hat{c}_k$ are the true and estimated concentrations of the analyte in the kth standard or unknown.

Results and discussion

Parallel factor analysis (PARAFAC) has become a popular method for EEM analysis and been employed for decomposition of multi-linear data arrays since it was developed by R. A. Harshman.[31] Trilinear data is the most common example of multi-linear data being generated and examined today. With the increasing number of analytical instruments capable of producing this type of data,[32,33] application of multi-linear decomposition methods, such as PARAFAC, is growing. Mathmatically, the trilinear model is expressed as in eqn. (2),

$$x_{ijk} = \sum_{r=1}^{R} \hat{a}_{ir}\hat{b}_{jr}\hat{c}_{kr} + e_{ijk} \qquad (2)$$

where x_{ijk} is the ijk^{th} element of the $I \times J \times K$ three-way data array X, $\hat{a}_{ir}$, $\hat{b}$IRjr and $\hat{c}_{kr}$ are the ith, j^{th} and k^{th} row of the rth column of the estimated factor loading matrices $\hat{\mathbf{A}}$, $\hat{\mathbf{B}}$ and $\hat{\mathbf{C}}$, R is the rank the model and e_{ijk} is the error in the model. The PARAFAC algorithm decomposes trilinear data in to R sets of triads, which make up the matrices $\hat{\mathbf{A}}$, $\hat{\mathbf{B}}$ and $\hat{\mathbf{C}}$ with the dimensions $I \times R$, $J \times R$ and $K \times R$, respectively. The matrices $\hat{\mathbf{A}}$, $\hat{\mathbf{B}}$ and $\hat{\mathbf{C}}$ are iteratively estimated using an alternating least squares (ALS) procedure until convergence. Convergence is achieved when the difference between successive estimates of $\hat{\mathbf{A}}$, $\hat{\mathbf{B}}$ and $\hat{\mathbf{C}}$ is sufficiently small that the model is nearly identical for subsequent iterations. The uncorrected correlation coefficient[34] was employed as the convergence criterion, with convergence being defined as when the difference between successive iterations was less than 10^{-9}. A detailed explanation of the PARAFAC algorithm may be found in a tutorial by R. Bro.[35]

A significant advantage of the trilinear model *versus* the bilinear model is that the solution is rotationally unique when each factor is linearly independent, the correct number of factors is chosen and the minimum of I, J, or K is greater than or equal to the rank of the model, R.[36] However, J. B. Kruskal showed that the third constraint is too strong and that a unique solution may exist when eqn. (3) is satisfied.[37]

$$k_A + k_B + k_C \geqslant 2R + 2 \qquad (3)$$

where k_A, k_B and k_C, are the k-ranks[36] of the factor loading matrices $\hat{\mathbf{A}}$, $\hat{\mathbf{B}}$ and $\hat{\mathbf{C}}$, respectively. For example, the k-rank of the factor loading matrix, $\hat{\mathbf{A}}$, is the minimum of I, the number of variables in the first dimension of the three-way data array X, or R, the rank of the model (eqn. (4)).

$$k_A = \min(I,R) \qquad (4)$$

The k-ranks of $\hat{\mathbf{B}}$ and $\hat{\mathbf{C}}$ are determined in a similar manner. Under these conditions, the resolved factors represent the true physical profiles of each component. For example, analysis of a set of samples using a HPLC with UV/VIS-DAD would produce an absorbance, chromatographic and concentration profile for each analyte. This result permits the estimation of more components than the limiting number of variables in each dimension.

In traditional EEM spectroscopy, the excitation resolution is often quite high; there is no redundancy in the excitation wavelengths from channel to channel. In contrast, excitation wavelength regions can overlap when using LEDs, due to their broad wavelength ranges. This is especially true when trying to maximize excitation spectral coverage. The excitation overlap in LED-EEM spectroscopy need only be reduced as required to resolve analytes of interest. As we will show, even closely related analytes are distinguishable using a general purpose LED array which included some spectrally overlapped excitation wavelengths. A more specific selection of LEDs can be used to better resolve a particular sample. This is analogous to moving or selecting a different grating in an excitation spectrograph.

The LED-EEM system has proven capable for the analysis of complex mixtures of fluorescent analytes. The optical output stability of the LED array, recorded during the four days in which these measurements were made, was excellent. The mean area of scattered light peaks generated by the standard scattering solution (glycogen) varied by less than 5% for all seven LEDs, over the entire four day measurement period. Excitation variations with a lamp source require instantaneous correction (quantum counting channel in a fluorimeter) or limiting data collection to a period in which the variation is acceptable. These considerations have been found to be unnecessary using the LED excitation system.

A comparison of instrumental sensitivity was performed by measuring rhodamine B fluorescence in ethanol at 0.0, 12.5, 25.0, 50.0 and 100.0 ppb, at the excitation maximum on each instrument at a common emission wavelength maximum of 564 nm. The fluorimeter had excitation and emission resolution of 2 nm, and the LED was driven at 2.98 V producing 108 μW of average optical power. The fluorimeter maximally excited rhodamine B at 542 nm *versus* the LED system recording the maximum excitation of rhodamine B using the 505 nm LED. The lower LED excitation wavelength is due to both the broad emission spectrum of the 505 nm LED and the lower excitation

energy available with the 530 nm LED (refer to Table 1). The LOD were obtained from univariate calibration curves using the fluorescence emission intensity at 564 nm from the fluorimeter and LED-EEM system. The rhodamine B LOD for the LED system was 0.70 ppb and the LOD for the conventional fluorimeter was 0.08 ppb, a factor of 8.8 greater. This result is quite good, considering the cost of a conventional fluorimeter's excitation source and that of the LED array. Furthermore, the excitation energy used in this experiment is considerably lower than that obtainable if the LEDs were driven at a higher voltage; the LOD is artificially high with respect to the capability of the LED.

During analysis of the fluorescein standards, the true power of the multi-way data collected with the LED-EEM instrument and the corresponding analysis was made abundantly clear. The analysis of a single component fluorescein solution resulted in two distinct factors to describe the fluorescein emission. The fluorescence of 200 ppb fluorescein in ethanol at the LED excitation wavelengths is shown in Fig. 4. As can be seen, there is variation in the emission peaks as a function of excitation wavelength indicating the presence of more than one component. The fluorescence spectrum is broader at lower excitation wavelengths with a maximum at 520 nm and shoulder around 550 nm. At higher excitation wavelengths the shoulder disappears resulting in a single maximum at 520 nm. Upon PARAFAC analysis, using three factors, the emission of both anionic forms of fluorescein were resolvable as given in Fig. 5. It is clear from the resolved components that two distinct species are fluorescing. In Fig. 5a, the monoanion (I) was maximally excited at 430 nm *versus* the maximum excitation of the dianion (II) at 505 nm. Similarly, in Fig. 5b, the emission maximum for the dianion (II) was 520 nm *versus* two maxima for the monoanion (I) at 515 nm and 535 nm. The third factor, while somewhat elevated, is dominated by noise and describes the instrumental background. These two forms of fluorescein have been observed (by spectral subtraction) and studied in the literature; our spectra are in agreement with the published data.[38] It is well known that only the dianion form of fluorescein is present in basic solutions. A 200 ppb solution of fluorescein in basic ethanol showed the emission spectra were independent of excitation wavelength, confirming that the two factors represent two fluorescent forms of fluorescein present in neutral environments. The contributions of the mono- and dianion forms of fluorescein were resolved *a priori*, as they cannot be obtained individually and exist in solution only. This example demonstrates the power of the LED-EEM system combined with PARAFAC analysis.

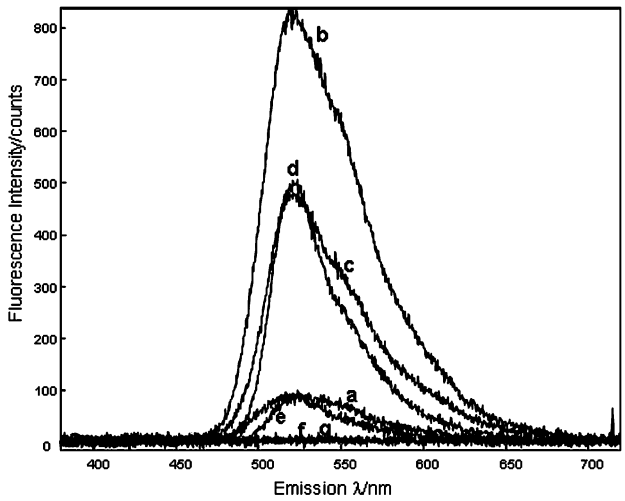

Fig. 4 Fluorescence spectra of 100 ppb fluorescein in ethanol collected simultaneously at LED wavelengths (a) 370 nm, (b) 430 nm, (c) 470 nm, (d) 505 nm, (e) 530 nm, (f) 590 nm, and (g) 636 nm.

To further characterize and test the instrument, two to six component mixtures of dyes in ethanol were measured and analyzed. The ability of the system to resolve a wide variety of components and closely related species is well demonstrated using these two to six component samples. The dyes were chosen to illustrate the range of molecules detectable using an LED array EEM instrument, but also to show the ability to resolve overlapping spectra. The resolved excitation and emission profiles of the six components are given in Fig. 6. The full emission wavelength range is used, and several components are significantly overlapped: rhodamine B and fluorescein, and 9,10-bis(phenylethynyl)-anthracene and fluorescein. In Fig. 6a, there is significant excitation overlap, with rhodamine B and safranin O having almost identical LED excitation and emission spectra. However, the slight differences in the LED-excitation and emission spectra allow resolution and quantitation of both rhodamine B and safranin O. The effect of the broad LED wavelength range can be seen in the resolved excitation profiles of the six components. The excitation spectra of the dyes are weighted with respect to the LEDs with the broadest excitation ranges (470 nm, 73 nm FWHM and 505 nm, 47 nm FWHM).

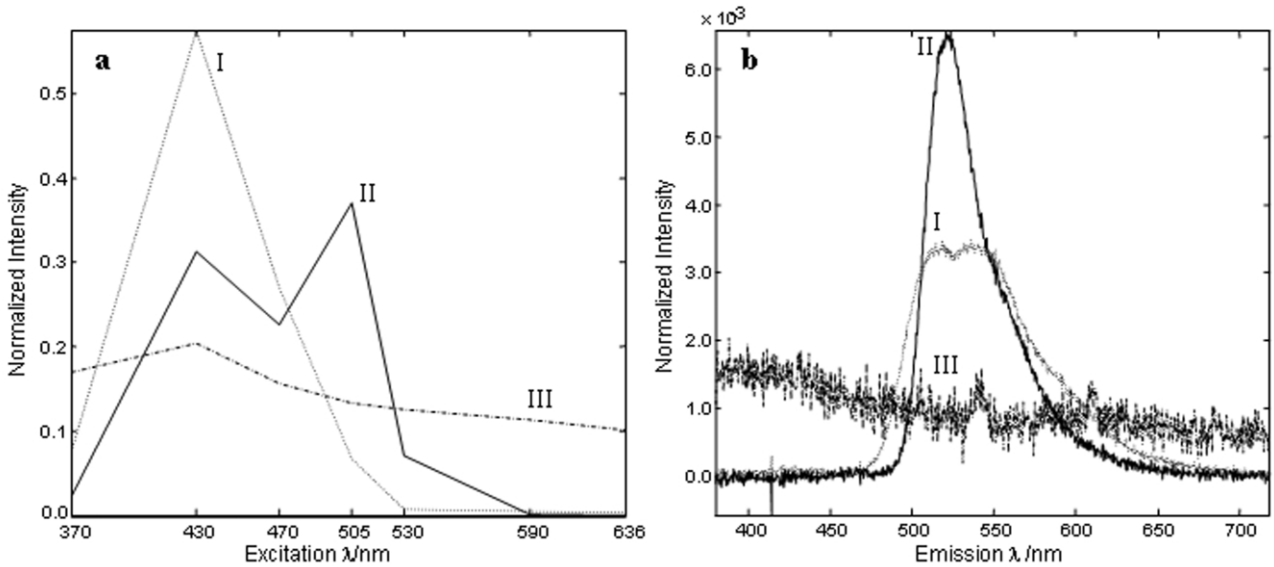

Fig. 5 PARAFAC model of fluorescein in ethanol using 3 factors: resolved (a) excitation and (b) emission spectra. I = fluorescein monoanion factor, II = fluorescein dianion factor, and III = instrumental background factor.

The figures of merit for the analysis of both the single component standards and multi-component mixtures are listed in Table 2. The PARAFAC resolved concentration profiles were used to build the calibration curves for quantitation described in Table 2. The total fluorescein concentration should be proportional to both the monoanion and dianion tautomers. However, fluorescein was quantified using only the predicted fluorescence of the monoanion due to the better linearity and sensitivity for this species. The RMSEC and correlation coefficient (r^2) show that the instrument is capable of precise calibration with RMSEC better than 4 ppb and r^2 values greater than 0.98. The LOD were less than 4 ppb with the best cases being in the mid ppt range. The quantitative capabilities of the instrument are good as given by the RMSEP. The RMSEP were less than 4 ppb for all analytes and were in the sub ppb range for 9,10-bis(phenylethynyl)-anthracene and rhodamine B.

Conclusions

An inexpensive, low electrical power light source consisting of individual LEDs has been developed for multi-way fluorescence applications using long wavelength UV and visible excitation light. The instrument was capable of resolving completely overlapped spectra of two anionic forms of fluorescein. Quantitative analysis was achieved with RMSEP values less than 4 ppb for all samples. Using LEDs often means lower excitation resolution and sometimes overlap in the excitation dimension due to the broad wavelength range (14–73 nm FWHM). However, the continuous wavelength coverage and unique excitation properties of each LED allows excitation of all analytes in the spectral range and full resolution of complex mixtures. The extent to which excitation and emission resolution or other parameters can be sacrificed while maintaining the requisite analytical information warrants further study.

With the ever increasing industrial and commercial demand for small, low power, and inexpensive UV light sources, deeper UV LEDs may become available. Recall, it was only relatively recently that we were awaiting the widespread availability of the then elusive blue LED (470 nm). Currently, we find ourselves two iterations deeper into the blue and UV: 430 nm and 370 nm, readily available from multiple vendors. Just prior to submission we discovered one vendor offering a 350 nm, 5 mm diameter LED with a power output of 30 μW distributed over a 30° viewing angle.[39] An important approach to using such a low power LED may involve direct coupling of LED light into the analytical sample thus avoiding the light losses associated with lenses.

Future research will possibly focus on developing a fiber optically coupled version of the LED-EEM instrument for front surface measurement of opaque samples such as soil, crude oil,[40] biomass, or tissue. This type of instrument may also be useful in endoscopic evaluations of certain cancers.[41] Other future directions include the development of a combined light source using a small inexpensive lamp source with filters for deep UV excitation and LEDs for visible through NIR excitation. Further studies of the sensor approach to EEM spectroscopy will shed light on the limitations and instrumental simplifications possible without sacrificing essential analytical capabilities.

Acknowledgements

The authors would like to acknowledge the Office of Naval Research and the Naval Research Laboratory for funding this

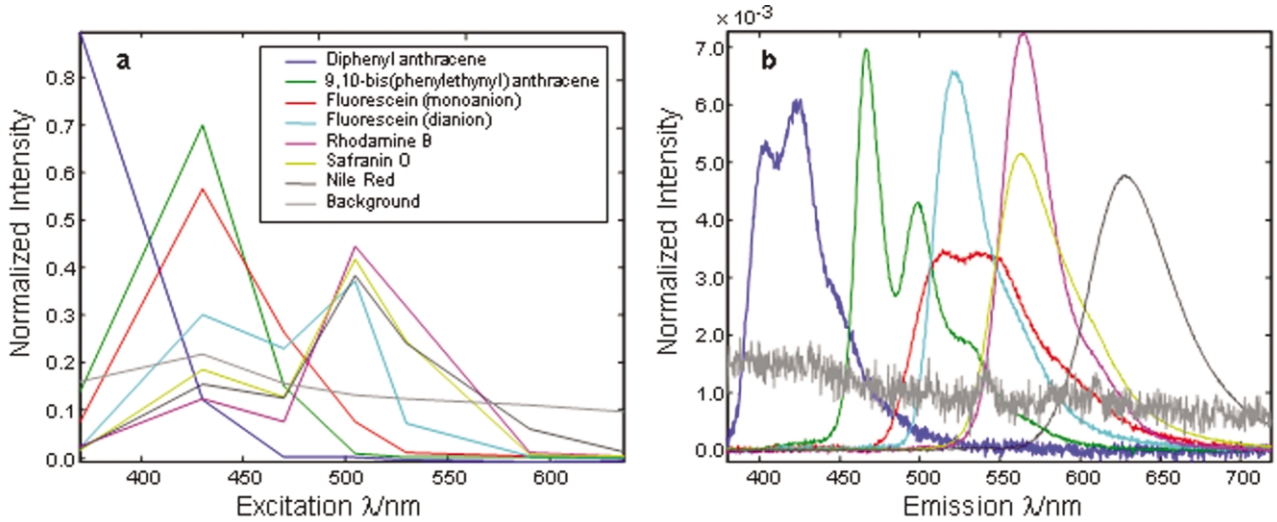

Fig. 6 PARAFAC model of the 6 components using 8 factors: resolved (a) excitation and (b) emission spectra.

Table 2 Figures of merit for quantitation of the dye standards and unknowns

Analyte	Concentration range (ppb)	Sensitivity (counts per ppb)	LOD (ppb)	RMSEC[a] (ppb)	RMSEP[b] (ppb)	r^2
Diphenyl anthracene	62.5–500.0	1.25E + 02	3.68	0.30	1.67	0.999
10-bis(phenylethynyl) anthracene	12.5–100.0	2.13E + 03	0.53	0.10	0.18	0.996
Fluorescein (monoanion)	25.0–200.0	1.21E + 03	1.57	0.30	3.99	0.991
Rhodamine B	12.5–100.0	2.80E + 03	0.76	0.23	0.60	0.980
Safranin O	50.0–400.0	1.18E + 03	2.53	0.39	1.30	0.996
Nile Red	25.0–200.0	2.16E + 03	0.72	0.20	2.13	0.996

[a] Root mean squared error of calibration [b] Root mean squared error of prediction.

research. Renée JiJi acknowledges the support of the National Research Council and the Naval Research Laboratory through the NRC-NRL postdoctoral fellowship.

References

1 L. W. Hershberger, J. B. Callis and G. D. Christian, *Anal. Chem.*, 1981, **53**, 971.
2 B. Skoropinski, J. B. Callis, J. D. S. Danielson and G. D. Christian, *Anal. Chem.*, 1986, **58**, 2831.
3 R. Jalkian and B. Denton, *Proc. SPIE*, 1989, **1054**, 91.
4 K. S. Booksh and B. R. Kowalski, *Anal. Chem.*, 1994, **66**, A782.
5 A. R. Muroski, K. S. Booksh and M. L. Myrick, *Anal. Chem.*, 1996, **68**, 3534.
6 A. R. Muroski, K. S. Booksh and M. L. Myrick, *Anal. Chem.*, 1996, **68**, 3539.
7 K. S. Booksh, R. D. JiJi and G. A. Cooper, *Anal. Chim. Acta*, 1999, **397**, 61.
8 H. G. Lohmannsroben and L. Schober, *Appl. Opt.*, 1999, **38**, 1404.
9 S. J. Hart, G. J. Hall and J. E. Kenny, *Anal. Bioanal. Chem.*, 2002, **372**, 205.
10 K. S. Booksh and R. D. JiJi, *Anal. Chem.*, 2000, **72**, 718.
11 J. V. Sweedler, *Crit. Rev. Anal. Chem.*, 1993, **24**, 59.
12 S. J. Hart, Y. M. Chen, B. K. Lien and J. E. Kenny, *Proc. SPIE*, 1996, **2835**, 73.
13 S. J. Hart, Y. M. Chen, B. K. Lien, T. W. Best and J. E. Kenny, *Field. Anal. Chem. Tech.*, 1997, **6**, 25.
14 J. W. Pepper, A. O. Wright and J. E. Kenny, *Spectrochim. Acta A*, 2002, **58**, 317.
15 S. Wang, X. Huang, Z. Fang and P. K. Dasgupta, *Anal. Chem.*, 2001, **73**, 4545.
16 K. Uchiyama, W. Xu and J. Q. T. Hobo, *Fresenius' J. Anal. Chem.*, 2001, **371**, 209.
17 P. K. Dasgupta, Z. Genfa, L. Jianzhong, C. B. Boring, S. Jambunathan and R. Al-Horr, *Anal. Chem.*, 1999, **71**, 1400.
18 S. J. Hart, G. J. Hall and J. E. Kenny, *Proc. SPIE*, 1999, **3534**, 601.
19 A. Baker, *Environ. Sci. Technol.*, 2002, **36**(7), 1377.
20 C. E. Del Castillo, P. G. Coble, J. M. Morell, J. M. Lopez and J. E. Corredor, *Mar. Chem.*, 1999, **66**, 35.
21 L. Moberg, G. Robertsson and B. Karlberg, *Talanta*, 2001, **54**, 161.
22 R. Henrion, G. Henrion, M. Bohme and H. Behrendt, *Fresenius' J. Anal. Chem.*, 1997, **357**, 522.
23 G. Albrecht-Buehler, *Exp. Cell Res.*, 1996, **236**, 43.
24 P. L. Smart and I. M. S. Laidlaw, *Water Resour. Res.*, 1977, **13**(1), 15.
25 R. G. Lyons, *J. Hydrol.*, 1993, **152**(1–4), 13.
26 F. Ricchelli and S. Gobbo, *J. Photochem. Photobiol. B*, 1995, **29**(1), 65.
27 J. H. Aiken, C. W. Huie and J. A. Terzian, *Anal. Lett.*, 1994, **27**(3), 511.
28 M. A. Bowers, L. D. Aicher, H. A. Davis and J. S. Woods, *J. Lab. Clin. Med.*, 1992, **120**(2), 272.
29 J. C. Ng, L. X. Qi and M. R. Moore, *Cell. Mol. Biol.*, 2002, **48**(1), 111.
30 K. S. Booksh, http://www.public.asu.edu/~booksh/chemometrics_course.htm, accessed URL 6/11/02.
31 R. A. Harshman, *UCLA Working Papers in Phonetics*, 1970, **16**, 1.
32 T. Hirschfeld, *Anal. Chem.*, 1980, **52**(2), 297A.
33 I. M. Warner, G. Patonay and M. P. Thomas, *Anal. Chem.*, 1985, **57**(3), 463A.
34 B. C. Mitchell and D. S. Burdick, *Chemom. Intell. Lab.*, 1993, **20**, 149.
35 R. Bro, *Chemom. Intell. Lab.*, 1997, **38**, 149.
36 R. A. Harshman and M. E. Lundy, in *Research Methods for Multimode Data Analysis*, ed. H. G. Law, C. W. Snyder, J. A. Hattie and R. P. McDonald, Praeger Publishers, New York, 1984, 122–215.
37 J. B. Kruskal, in *Multiway Data Analysis*, ed. R. Coppi and S. Bolasco, Elsevier Science Publishers B. V. (North Holland), Amsterdam, 1989, 7–18.
38 N. Klonis and W. H. Sawyer, *Photochem. Photobiol.*, 2000, **72**(2), 179.
39 Roithner Lasertechnik, http://www.roithner-laser.com/LED_diverse.htm, accessed URL 6/11/02.
40 O. C. Mullins, T. Daigle, C. Crowell, H. Groenzin and N. B. Joshi, *Appl. Spectrosc.*, 2001, **55**(2), 197.
41 K. T. Moesta, B. Ebert, T. Handke, D. Nolte, C. Nowak, W. E. Haensch, R. K. Pandey, T. J. Dougherty, H. Rinneberg and P. M. Schlag, *Cancer Res.*, 2001, **61**(3), 991.